

A phosphorelay system controls stalk biogenesis during cell cycle progression in *Caulobacter crescentus*

Emanuele G. Biondi,[†] Jeffrey M. Skerker,[†]
Muhammad Arif, Melanie S. Prasol, Barrett S. Perchuk
and Michael T. Laub*

Bauer Center for Genomics Research, Harvard University,
7 Divinity Avenue, Cambridge, MA 02138, USA.

Summary

A fundamental question in developmental biology is how morphogenesis is coordinated with cell cycle progression. In *Caulobacter crescentus*, each cell cycle produces morphologically distinct daughter cells, a stalked cell and a flagellated swarmer cell. Construction of both the flagellum and stalk requires the alternative sigma factor RpoN (σ^{54}). Here we report that a σ^{54} -dependent activator, TacA, is required for cell cycle regulated stalk biogenesis by collaborating with RpoN to activate gene expression. We have also identified the first histidine phosphotransferase in *C. crescentus*, ShpA, and show that it too is required for stalk biogenesis. Using a systematic biochemical technique called phosphotransfer profiling we have identified a multicomponent phosphorelay which leads from the hybrid histidine kinase ShkA to ShpA and finally to TacA. This pathway functions *in vivo* to phosphorylate and hence, activate TacA. Finally, whole genome microarrays were used to identify candidate members of the TacA regulon, and we show that at least one target gene, *staR*, regulates stalk length. This is the first example of a general method for identifying the connectivity of a phosphorelay and can be applied to any organism with two-component signal transduction systems.

Introduction

In many organisms, programs of morphogenesis and development are temporally coupled to cell cycle progression, yet the molecular basis of this coupling remains poorly understood, particularly in bacteria. *Caulobacter crescentus* has emerged as a tractable model system for studying the regulation of these fundamental processes

as cell cycle progression in this organism is accompanied by a series of morphological transitions culminating in the production of two distinct daughter cells, a swarmer cell and a stalked cell (Ohta *et al.*, 2000; Ryan and Shapiro, 2003; Skerker and Laub, 2004). Motile swarmer cells possess a single polar flagellum and polar pili, and they cannot initiate DNA replication. Swarmer cells differentiate into stalked cells by shedding their polar flagellum, retracting the pili, and synthesizing a stalk at the former site of the flagellum. This motile-to-sessile transition accompanies a G1-S transition and the initiation of a single round of DNA replication. During the ensuing S-phase and a brief G2 phase, the predivisional cell continues to extend the polar stalk, while also building a new polar flagellum and pili opposite the stalked pole. An asymmetric cell division then ensues, producing a new swarmer and new stalked cell (see also Fig. 7).

The polar stalk of *Caulobacter* has been suggested to serve a number of important functions. The adhesive polysaccharide substance called holdfast at the distal tip of the stalk allows cells to bind to abiotic surfaces or to other cells (Poindexter, 1964; Kurtz and Smit, 1994; Smith *et al.*, 2003). As *Caulobacter* is an aquatic, aerobic bacterium, the stalk has also been suggested to affect buoyant density and help cells stay associated with the air-water interface (Poindexter, 1978). Finally, the stalk may play a significant role in nutrient acquisition. Cells starved for phosphate extend their stalks up to 10 or 20 times the length of the cell body, possibly as a mechanism to increase surface area and nutrient uptake ability (Poindexter, 1964; 1984; Gonin *et al.*, 2000).

Little is known about the regulation of stalk biogenesis. However, many other regulatory processes central to cell cycle progression and morphogenesis in *Caulobacter* are carried out by two-component signal transduction systems (Ohta *et al.*, 2000; Skerker and Laub, 2004). These signalling systems, comprised of histidine kinases and response regulators, are widespread in the prokaryotic kingdom, as well as being found in plants, yeast and slime moulds (Hoch and Silhavy, 1995). The *Caulobacter* genome encodes 62 histidine kinases and 44 response regulators (Nierman *et al.*, 2001; Skerker *et al.*, 2005). The canonical view of these signalling systems involves a sensor histidine kinase which autophosphorylates on a conserved histidine residue and then transfers the phosphoryl group to an aspartate residue on the receiver

Accepted 19 October, 2005. *For correspondence. E-mail laub@cgr.harvard.edu; Tel. (+1) 617 384 9647; Fax (+1) 617 495 2196. [†]These authors contributed equally to this work.

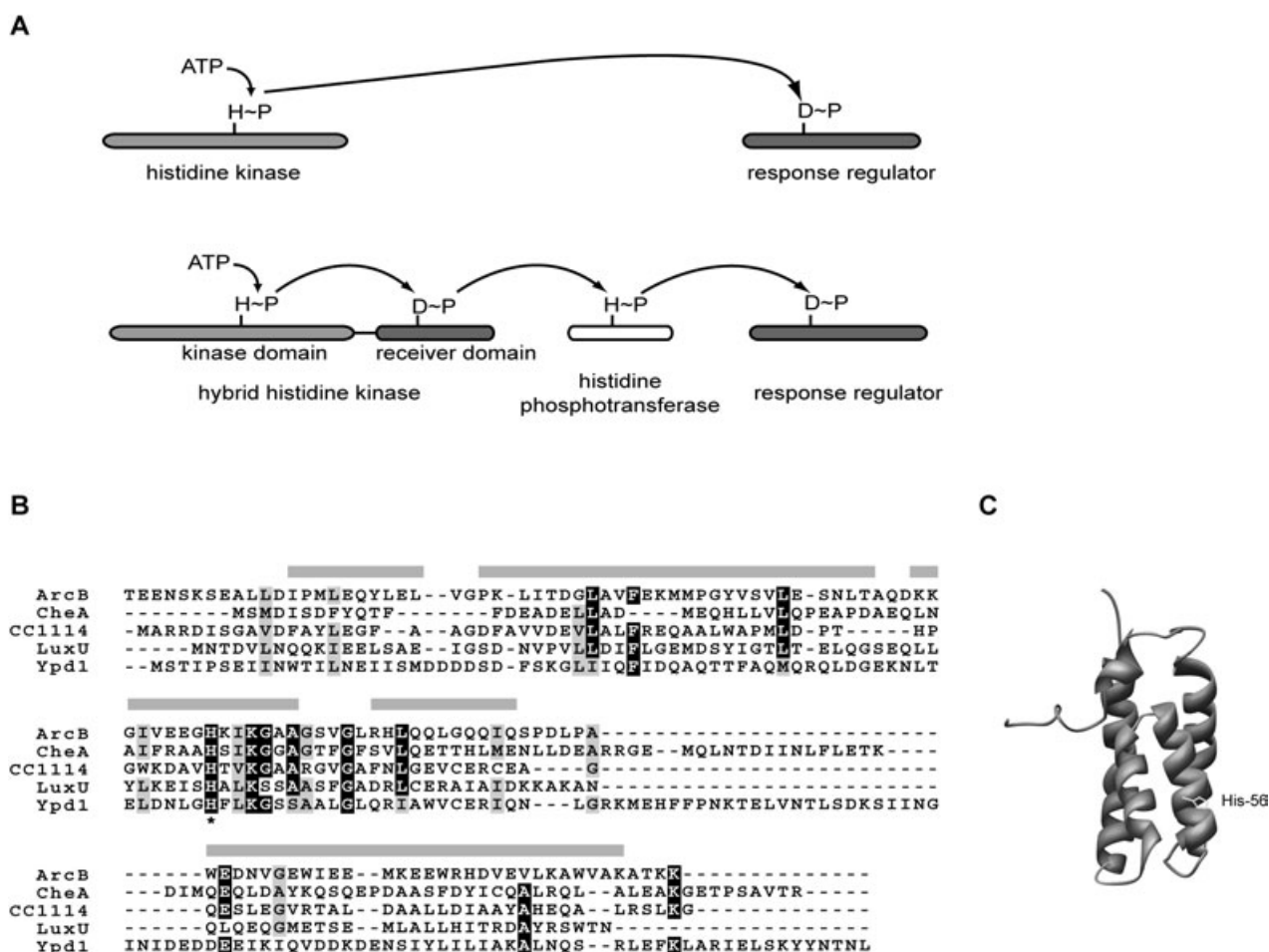


Fig. 1. Identification of a putative histidine phosphotransferase in *C. crescentus*.

A. Schematic of a canonical two-component signal transduction pathway versus a multicomponent phosphorelay.

B. CC1114 amino acid sequence was aligned against the phosphotransferase domain of ArcB (gi48994928, fragment 655–778 aa), the P1 domain of CheA (gi16129840, fragment 1–140 aa), LuxU (gi39721593) and Ypd1 (gi6319966), using 3D-Coffee. Alpha helices are indicated (grey bars) according to the secondary structure of ArcB.

C. Homology model of CC1114 using ArcB as template.

domain of a response regulator (Fig. 1A). Phosphorylation of the receiver domain activates the output domain, which often has the ability to bind DNA, thereby coupling signaling pathways to changes in gene expression and the execution of various cellular events.

Complicating this simple paradigm for two-component signalling are hybrid histidine kinases in which a histidine kinase contains a response regulator receiver domain at its C-terminal end. These hybrid histidine kinases often participate in more complex pathways called phosphorelays (Fig. 1A). In such pathways, hybrid kinases first autophosphorylate on a conserved histidine residue in the kinase domain and then transfer the phosphoryl group intramolecularly to a conserved aspartate in its receiver domain. The phosphoryl group is then transferred to another conserved histidine on a protein called a histidine phosphotransferase, which can in turn transfer its phos-

phoryl group to an aspartate on a diffusible response regulator. Unlike histidine kinases and response regulators, histidine phosphotransferases show little sequence identity to one another, with conservation of only a few critical residues and a four-helix bundle structure (Kato *et al.*, 1997; Song *et al.*, 1999; Xu and West, 1999).

Previous genetic screens as well as a systematic deletion of each of the 106 two-component genes in *Caulobacter* have identified 39 genes which are required for normal cell cycle progression or morphogenesis (Skerker *et al.*, 2005). Of these, 19 were impaired in motility and nine had defects in stalk biogenesis. Many of those involved in motility had been previously identified as regulators of flagellar biogenesis, the best understood aspect of morphogenesis in *Caulobacter*. The assembly of the polar flagellum in predivisional cells is controlled by a four-tiered transcriptional cascade (Ramakrishnan *et al.*, 1994;

Gober and England, 2000). This cascade is set in motion by the DNA-binding response regulator CtrA (Quon *et al.*, 1996). The phosphorylation and activity of CtrA are under extensive cell cycle control, coupling flagellar biogenesis to cell cycle progression (Quon *et al.*, 1996; Domian *et al.*, 1997). CtrA directly regulates the expression of at least 95 genes, including *rpoN*, which encodes the σ^{54} subunit of RNA polymerase (Laub *et al.*, 2002). *rpoN* mutants are non-motile and stalkless, suggesting that σ^{54} regulates genes involved in flagellum and stalk biogenesis (Brun and Shapiro, 1992).

σ^{54} -dependent gene expression typically requires a phosphorylated transcriptional activator of the NtrC-family of response regulators (Kustu *et al.*, 1989). In *Caulobacter*, *flbD* encodes a σ^{54} -dependent activator which is induced at approximately the same time as *rpoN*, and together with RpoN, activates expression of genes required late in flagellar assembly (Ramakrishnan *et al.*, 1991). FlbD also represses genes required early in flagellar assembly, and thus coordinates the timing of multiple steps in flagellum assembly (Wingrove *et al.*, 1993; Benson *et al.*, 1994; Wingrove and Gober, 1994). However, unlike *rpoN*, *flbD* mutants are not impaired in stalk synthesis, suggesting that another NtrC-like response regulator functions with *rpoN* to regulate stalk biogenesis.

In a systematic deletion of two-component signalling genes the NtrC-like regulator *tacA* was found to lack stalks (Skerker *et al.*, 2005), suggesting it regulates stalk biogenesis. In that study and previous genetic screens, deleting the histidine kinase *pleC* was also found to produce stalkless cells (Sommer and Newton, 1989; Skerker *et al.*, 2005). PleC, however, exclusively phosphorylates the response regulators DivK and PleD, and not TacA (Skerker *et al.*, 2005). In the systematic deletion study no other deletions of canonical histidine kinases produced a stalkless phenotype. However, the hybrid kinase CC0138 was found to be stalkless, suggesting that a phosphorelay controls phosphorylation of the σ^{54} -activator TacA. Here, using genetics and a systematic biochemical method called phosphotransfer profiling, we describe the identification of ShpA, the first histidine phosphotransferase in *Caulobacter*, and demonstrate that it is central to a phosphorelay which regulates stalk biogenesis by controlling the activity of TacA. Using whole-genome DNA microarrays, we identify the likely target genes of TacA. Our results provide evidence for a transcriptional cascade that regulates stalk biogenesis and suggest a mechanism for the cell cycle timing of stalk synthesis.

Results

Identification of *C. crescentus* histidine phosphotransferases

A systematic study of all *C. crescentus* two-component

signalling genes identified two genes whose deletion produced stalkless cells, the gene CC0138 which encodes a hybrid histidine kinase and CC3315 which encodes a σ^{54} -dependent response regulator named TacA (Skerker *et al.*, 2005). The discovery of these mutants suggested that a phosphorelay may control stalk formation in *C. crescentus*. However, phosphorelays require histidine phosphotransferases to shuttle phosphoryl groups from hybrid kinases to response regulators (Fig. 1A), and none were identified in the initial annotation of the *C. crescentus* genome based on sequence homology methods (Nierman *et al.*, 2001). To identify putative phosphotransferases in the *C. crescentus* genome, we searched for genes predicted to encode proteins bearing other common features. Specifically, we sought proteins with (i) fewer than 250 amino acids, (ii) greater than 70% predicted alpha helical secondary structure, and (iii) the conserved motif HXXKG within a predicted alpha helix. Two genes satisfied these criteria, CC1114 and CC1220. This report focuses on the gene CC1114 which is predicted to encode a protein of 112 amino acids with high alpha helical content (Fig. 1B). The primary sequence of CC1114 was successfully threaded onto the known four-helix bundle structures of three monomeric histidine phosphotransferases: Ypd1 from *Saccharomyces cerevisiae* (Xu and West, 1999), LuxU from *Vibrio harveyi* (Ulrich *et al.*, 2005), and the phosphotransferase domain of ArcB from *Escherichia coli* (Kato *et al.*, 1997) (Fig. 1C). These threaded structural alignments further predicted that His-56 of CC1114 lies within the middle of an alpha helix and is solvent exposed. Homologues of CC1114 are found in the genomes of closely related alpha-proteobacteria (Fig. S1). In sum, these bioinformatic analyses suggested that CC1114 may encode a histidine phosphotransferase.

CC1114 has histidine phosphotransferase activity in vitro

To determine whether the CC1114 protein exhibits phosphotransferase activity, we tagged CC1114 with a His₆-tag and purified the protein by affinity chromatography to greater than 90% homogeneity. To determine whether CC1114 can receive a phosphoryl group from a hybrid histidine kinase, we incubated CC1114 with the purified kinase and receiver domains from each of four hybrid kinases which possess high *in vitro* activity: CC0138, CckA, CC3102 and CC3219. We used separate kinase and receiver domains for each hybrid kinase because full-length constructs had little to no activity (data not shown). Reactions were initiated by the addition of [γ -³²P]-ATP, incubated for 30 min, and then resolved by SDS-PAGE (Fig. 2A). In each reaction, radiolabel was incorporated into the kinase domain by autophosphorylation and subsequently transferred to the corresponding receiver domain. For the reactions with CC0138 and CC3102,

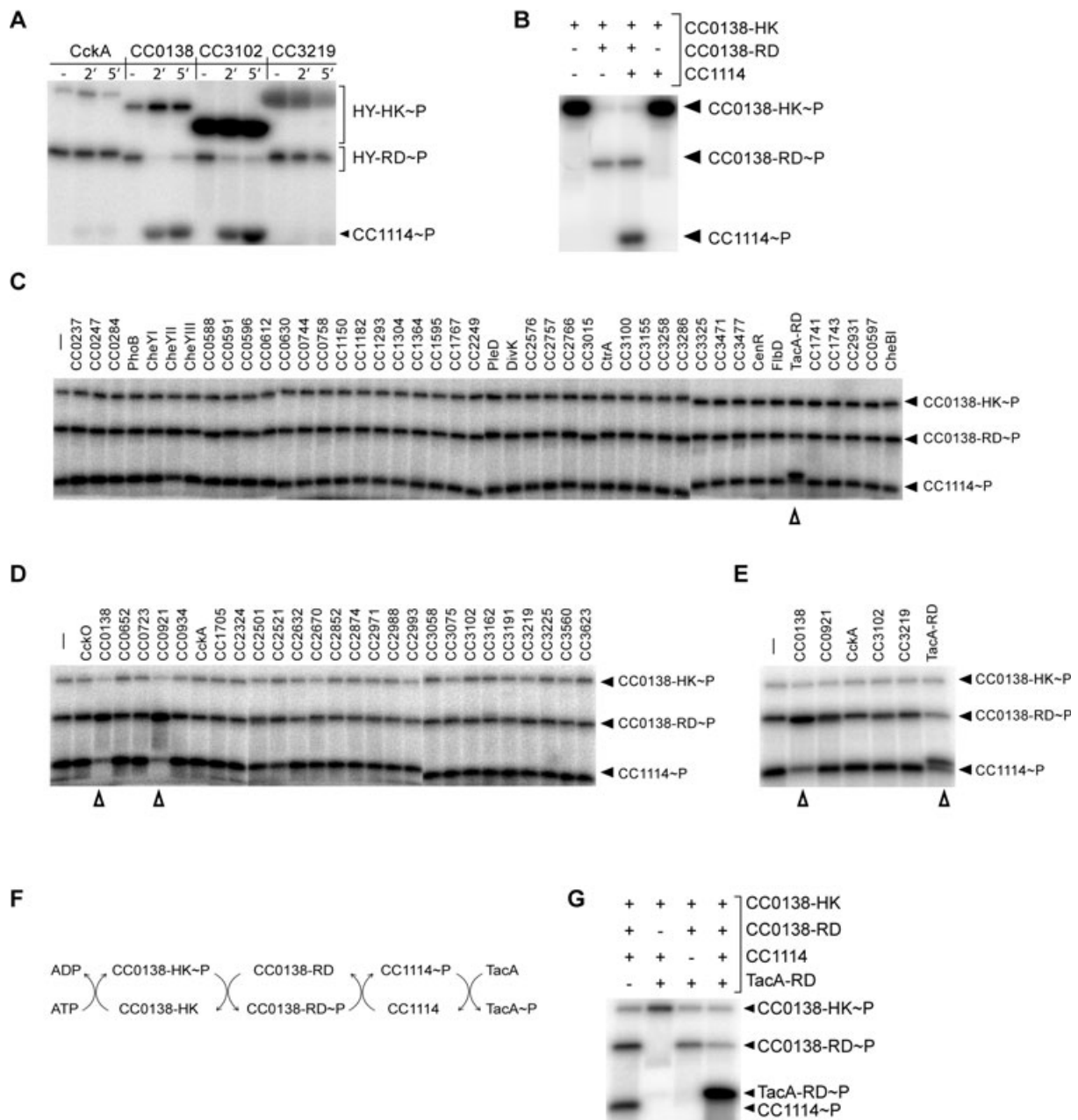


Fig. 2. Biochemical identification of the TacA phosphorelay.

A. CC1114 can be phosphorylated by *Caulobacter* hybrid kinases. The kinase (HY-HK) and receiver domains (HY-RD) for four different hybrid kinases were each purified and tested *in vitro* for their ability to phosphorylate CC1114. The gene name or CC number is indicated for each kinase. B. Phosphorylation of CC1114 is dependent on the presence of a receiver domain. Pluses and minuses indicate presence or absence of reaction components: purified kinase domain of CC0138 (CC0138-HK), its receiver domain (CC0138-RD), and CC1114. C and D. Identification of a CC1114-dependent phosphorelay using phosphotransfer profiling. Phosphorylated CC1114 was profiled against all 44 purified *Caulobacter* response regulators (C) and against all 27 purified receiver domains of *Caulobacter* hybrid kinases (D). Each phosphotransfer reaction was incubated for 2 min at room temperature. E. CC1114 exhibits a kinetic preference for CC0138 and TacA-RD. Phosphotransfer from CC1114 to the receiver domains of CC0138, CC0921, CckA, CC3102, CC3219 and TacA were tested at a 10 s time point. Open arrowheads in panels C–E indicate lanes with evidence of phosphotransfer, manifested as loss of radiolabel from the CC1114 band and/or incorporation of label on a receiver domain. F. Schematic of the phosphorelay between the hybrid kinase CC0138, the histidine phosphotransferase CC1114 and the response regulator TacA. G. Reconstitution of the phosphorelay *in vitro* using purified components. Pluses and minuses indicate the presence or absence of purified CC0138-HK, CC0138-RD, CC1114 and TacA-RD.

significant accumulation of label was also found at a position corresponding to CC1114. Incubation of CC1114 with the CC0138 kinase domain in the absence of the CC0138 receiver domain was indistinguishable from incubating the CC0138 kinase domain alone (Fig. 2B, lane 1 vs. 4) indicating that (i) the receiver domain is required for phosphotransfer from the kinase domain to CC1114, and (ii) CC1114 does not have autophosphorylation activity. Together these observations support the conclusion that CC1114 is a histidine phosphotransferase.

CC1114 participates in a phosphorelay culminating in the phosphorylation of TacA

We previously developed an assay called phosphotransfer profiling which allows the rapid, systematic identification of response regulator targets of a given histidine kinase (Skerker *et al.*, 2005). In this assay, one histidine kinase is systematically tested *in vitro* for its ability to transfer a phosphoryl group to each purified response regulator encoded in the genome. As histidine kinases exhibit a large kinetic preference *in vitro* for their *in vivo* cognate substrates, kinase-regulator pairs are easily identified by testing phosphotransfer at multiple time points and identifying the kinetically preferred substrate(s) (Skerker *et al.*, 2005). Here, we adapted this assay (also see Fig. S2) to examine the substrate specificity, and hence probable *in vivo* partners, of CC1114. CC1114 was first phosphorylated (producing CC1114-P) and then split and incubated individually for 2 min with each of the 44 purified, full-length response regulators encoded in the *C. crescentus* genome (Skerker *et al.*, 2005). Phosphorimaging demonstrated a single preferred target of CC1114-P, the response regulator TacA (Fig. 2C).

Next, we wished to identify the hybrid kinase which phosphorylates CC1114. *In vivo* hybrid histidine kinases can pass a phosphoryl group to a phosphotransferase or vice versa, with the directionality typically driven by mass-action (Uhl and Miller, 1996; Georgellis *et al.*, 1998). We took advantage of this reversibility to identify the hybrid kinases which interact with CC1114, by profiling phosphotransfer from CC1114-P to the purified receiver domains of each of the 27 hybrid kinases encoded in *C. crescentus* (Fig. S3). With phosphotransfer reaction times of 2 min, two receiver domains, from the hybrid kinases CC0138 and CC0921, were efficiently phosphorylated, resulting in depletion of radiolabel from CC1114-P (Fig. 2D). However, with a shorter reaction time (Fig. 2E), CC1114 exhibited a kinetic preference for phosphotransfer to the CC0138 receiver domain. Furthermore, the rate of transfer to the CC0138 and TacA receiver domains was approximately equal, suggesting that these are the kinetically preferred and hence most likely *in vivo* partners for CC1114 (Fig. 2E). Finally, as a control, we examined the

phosphotransfer profile of the CC0138 kinase domain with respect to each of the 44 soluble, full-length *C. crescentus* response regulators. This experiment verified that CC0138 does not directly phosphorylate TacA or any response regulator other than its own receiver domain (data not shown).

Taken together, the phosphotransfer profiles suggest that CC1114 mediates a phosphorelay between the hybrid kinase CC0138 and the response regulator TacA (Fig. 2F). To verify the complete biochemical pathway, we mixed all components with [γ - 32 P]-ATP and incubated reactions at 30°C (Fig. 2G). Phosphorimaging showed that label accumulated mostly in TacA (Fig. 2G, lane 4). Excluding the CC0138 receiver domain (Fig. 2G, lane 2) or CC1114 (Fig. 2G, lane 3) from the reaction eliminated phosphorylation of TacA. These data support the conclusion that autophosphorylation of CC0138 leads to a phosphorelay through its own receiver domain and CC1114, culminating in the phosphorylation of TacA.

CC0138, CC1114 and TacA control stalk biogenesis and cell division

The phosphotransfer experiments suggested that CC1114 mediates an exclusive phosphorelay which leads to phosphorylation of TacA. As deletion strains for both *tacA* and CC0138 were found previously to lack stalks (Skerker *et al.*, 2005), we predicted that a CC1114 deletion should also be stalkless. We therefore constructed a strain in which almost the entire coding region of CC1114 was replaced with a tetracycline resistance cassette. Examination of this strain by light microscopy confirmed that Δ CC1114, like Δ CC0138 and Δ *tacA*, is stalkless in rich (Fig. 3A, D, G and J) and minimal media (data not shown). However, deletion strains for each phosphorelay component were able to synthesize stalks when grown in low phosphate medium, a condition known to trigger extensive stalk growth (Poindexter, 1964; 1984; Gonin *et al.*, 2000), suggesting that these strains are impaired in the regulation of stalk biogenesis, not stalk synthesis *per se* (Fig. 3C, F, I and L). Each deletion strain also appeared mildly filamentous with at least 20% of cells showing obvious cellular elongation relative to wild type, suggesting a defect in cell division or control of cell growth. Motile cells of Δ CC0138, Δ CC1114 and Δ *tacA* were easily observed by microscopy, but due to elongation cells did not swim as rapidly as wild type. Consistent with this observation, each phosphorelay mutant showed partial defects in a swarm plate motility assay (Fig. 3M). Δ CC0138, Δ CC1114 and Δ *tacA* each exhibited a swarm size intermediate between that of the wild-type CB15N and the non-motile strains Δ *flbD* and *rpoN::Tn5*, presumably due to the inability of the filamentous, mutant cells to swim efficiently through the agar.

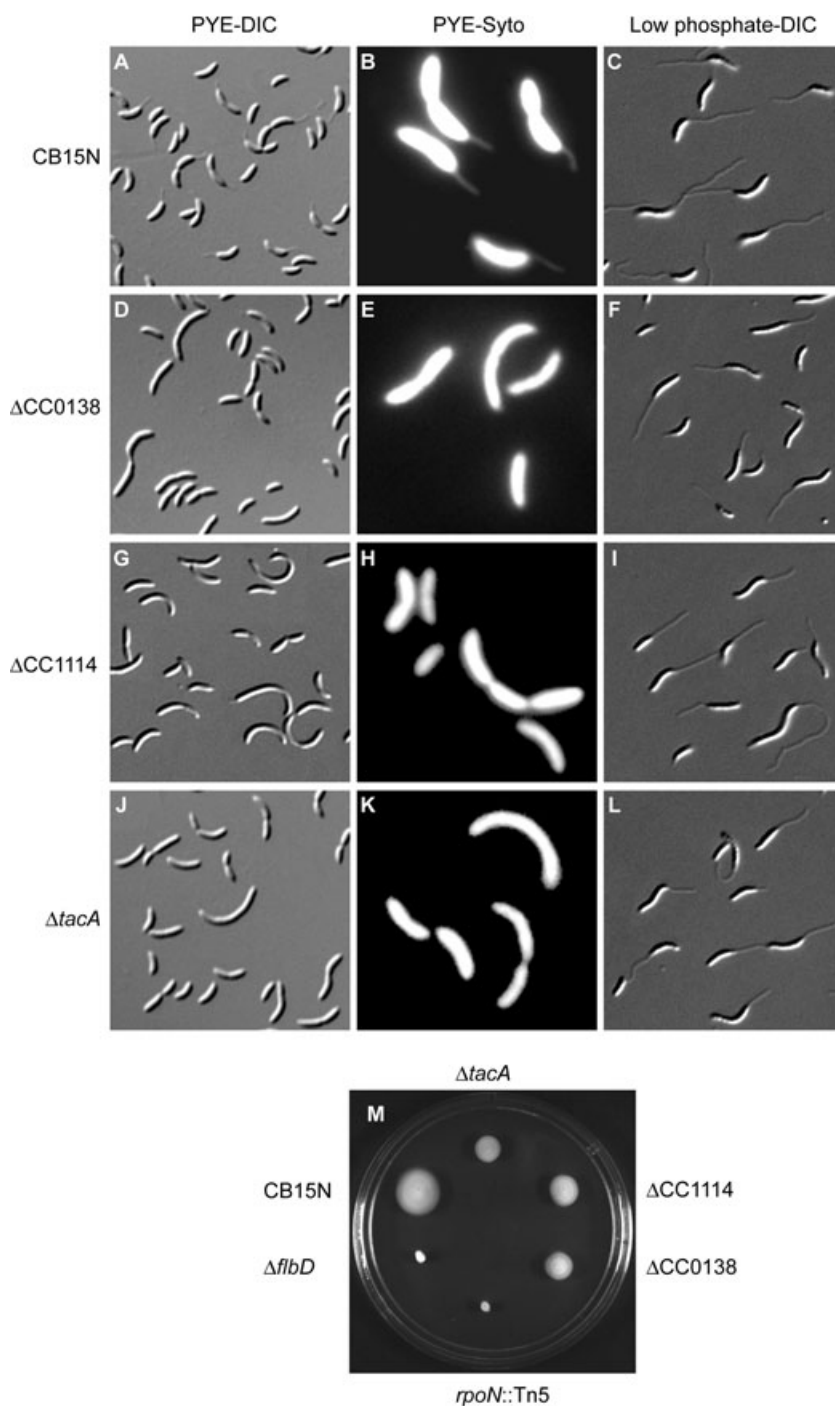


Fig. 3. Phenotypic characterization of Δ CC0138, Δ CC1114 and Δ tacA.

A, D, G, J. Differential interference contrast (DIC) images of wild-type CB15N (A), Δ CC0138 (D), Δ CC1114 (G) and Δ tacA (J) grown to mid-log phase in PYE medium.

B, E, H, K. Fluorescent images of CB15N (B), Δ CC0138 (E), Δ CC1114 (H) and Δ tacA (K) stained with Syto-9 to visualize stalks.

C, F, I, L. DIC images of CB15N (C), Δ CC0138 (F), Δ CC1114 (I) and Δ tacA (L), grown in low phosphate medium, showing long stalks in this growth condition.

M. Swarm plate analysis of wild-type and mutant strains. CB15N forms a large swarm at the point of inoculation. Δ flbD and $rpoN::Tn5$ are both non-motile control strains. Δ tacA, Δ CC1114 and Δ CC0138 are motile, but produce smaller swarms due to defects in cell division.

The mutant phenotypes of Δ CC0138, Δ CC1114 and Δ tacA were each complemented by providing the deleted gene on a plasmid (Fig. 4A, C and H), demonstrating that the cell division and stalk phenotypes were due to a single gene deficiency in each case. Δ CC1114 cannot however, be complemented by an allele of CC1114 bearing the H56A mutation (Fig. 4B), consistent with the prediction that His-56 is the sole phosphorylation site on CC1114.

Moreover, purified CC1114(H56A) also did not exhibit phosphotransferase activity *in vitro* (data not shown).

In sum, deleting any component of the CC0138-CC1114-TacA phosphorelay led to a minor defect in cell division or control of cell growth resulting in elongated cells, and a major defect in stalk biogenesis. As growth, division, and stalk biogenesis each involve the coordination of peptidoglycan and cell membrane metabolism

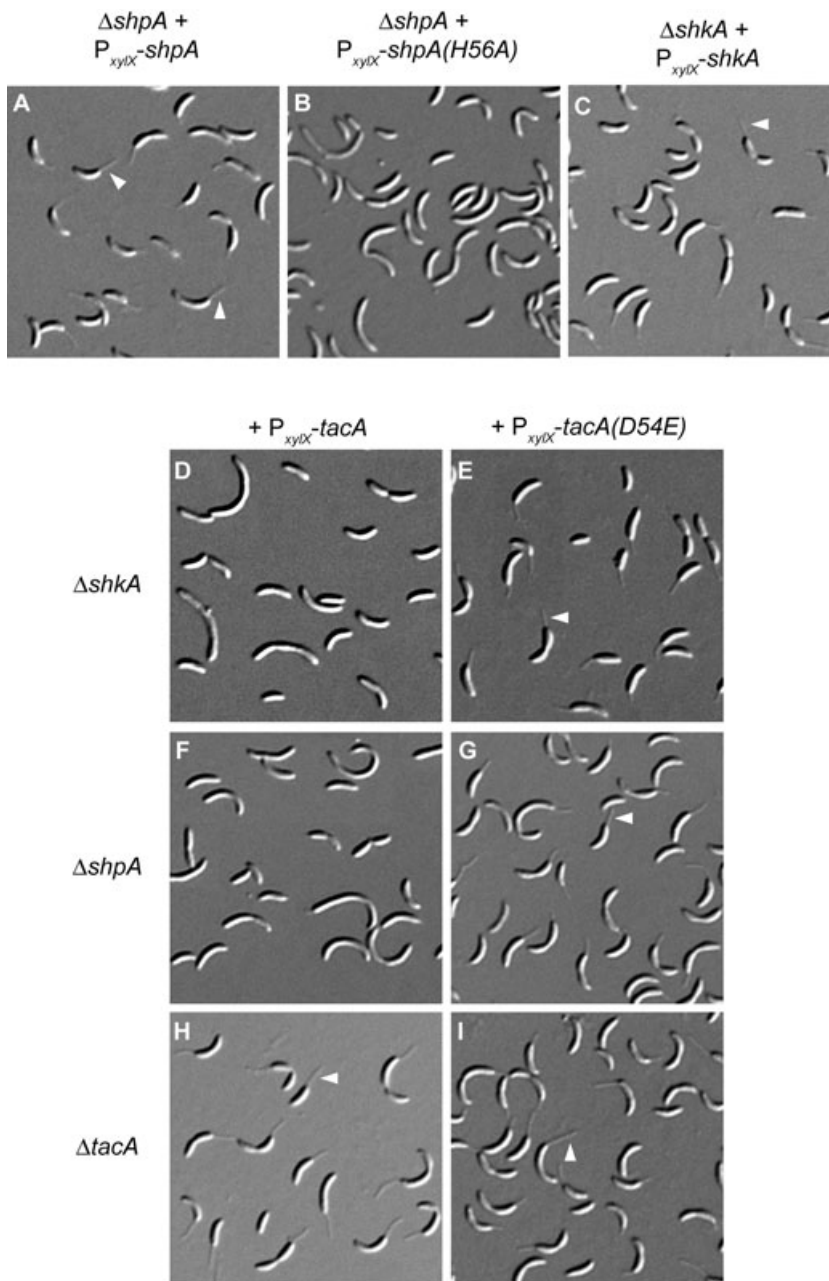


Fig. 4. Genetic analysis of the TacA phosphorelay. CC0138 = *shkA*, CC1114 = *shpA*.

A. Deletion of CC1114 results in a stalkless phenotype (Fig. 3G), which is complemented by providing a copy of the CC1114 gene *in trans* on the plasmid pHXM-CC1114 (ML691). The presence of stalks is indicated by white arrowheads.

B. CC1114 bearing a mutation of the active site histidine to an alanine (H56A) is unable to complement stalk formation *in vivo*.

A, C, H. Phosphorelay mutants can be complemented by providing the gene *in trans* on a xylose-inducible plasmid. (A) ML691 ($\Delta shpA$ + pHXM-*shpA*), (C) ML690 ($\Delta shkA$ + pHXM-*shkA*), (H) ML692 ($\Delta tacA$ + pHXM-*tacA*). All strains were grown in PYE + glucose, which provides a low level of expression of the gene being tested. Stalks are indicated by white arrowheads. DIC images of strains grown to mid-log phase.

D–I. Expression of *tacA(D54E)* but not *tacA*, is able to rescue the stalk defect of both $\Delta shkA$ (D vs. E) and $\Delta shpA$ (F vs. G). (H–I) Either *tacA* or *tacA(D54E)* can rescue a $\Delta tacA$ mutant.

(Wagner *et al.*, 2005), a single deficiency may underlie all of the morphological phenotypes of $\Delta CC0138$, $\Delta CC1114$ and $\Delta tacA$. Moreover, the similarity of mutant phenotypes for CC0138, CC1114 and *tacA* supports the notion that they act in the same signalling pathway *in vivo*, as suggested by the *in vitro* results demonstrating a phosphorelay comprised of these proteins. As the major defect of the deletion strains is in stalk biogenesis we have named CC0138 *shkA* for stalk biogenesis histidine kinase A and named CC1114 *shpA* for stalk biogenesis histidine phosphotransferase A.

The constitutively active allele *tacA(D54E)* rescues $\Delta shkA$, $\Delta shpA$ and $\Delta tacA$

The data presented thus far suggest that ShkA and ShpA function *in vivo* to phosphorylate TacA. We therefore predicted that expression of a constitutively active form of *tacA*, *tacA(D54E)*, should rescue deletion of *shkA* or *shpA*. In the NtrC family of response regulators, which includes TacA, changing the active site aspartate to a glutamate often mimics phosphorylation of the response regulator and hence renders its activation

independent of upstream kinases or phosphorelays (Klose *et al.*, 1993). We therefore placed a *tacA(D54E)* allele on the vector pJS71 under control of the xylose-inducible promoter P_{xyIX} (Meisenzahl *et al.*, 1997) and transformed this plasmid into the strains $\Delta shkA$, $\Delta shpA$ and $\Delta tacA$. Each strain was grown in rich medium supplemented with glucose. As the pJS71 vector is a relatively high copy vector, growth in the presence of the repressor glucose leads to a low level of expression from P_{xyIX} but prevents overexpression. For $\Delta shkA$, $\Delta shpA$ and $\Delta tacA$, expression of *tacA(D54E)* rescued both the cellular elongation and stalk defects of the mutant strains (Fig. 4E, G and I). In contrast, expression of wild-type *tacA* from the same plasmid rescued $\Delta tacA$ (Fig. 4H), but did not rescue the mutant phenotypes of $\Delta shkA$ or $\Delta shpA$ (Fig. 4D and F). Even overexpression of wild-type *tacA*, by growth in 0.1% xylose, did not rescue the $\Delta shkA$ and $\Delta shpA$ mutants (data not shown). These data support the conclusion that the primary *in vivo* function of ShkA and ShpA is to phosphorylate, and hence activate, TacA.

Next, we examined the effect of overproducing TacA(D54E). Wild-type cells harbouring the P_{xyIX} -*tacA(D54E)* allele on pJS71 were grown in the presence of either glucose or xylose. In glucose, these cells appeared wild type in terms of morphology (Fig. 5A) and growth rate (data not shown). However, in xylose the cells grew almost twice as slowly as in glucose and rapidly became filamentous. Cells had abnormal stalks that were shorter or longer than wild type and in some cases appeared only as a small bud or protrusion from the cell pole (Fig. 5B). These growth and stalk defects could be the result of high levels of constitutively active TacA and/or the synthesis of active TacA at the wrong time during cell cycle progression. Together, the overexpression and deletion analyses indicate that TacA activity must be tightly regulated during the *Caulobacter* cell cycle to ensure proper stalk biogenesis.

Identifying the TacA regulon with DNA microarrays

TacA is a member of the NtrC family of response regu-

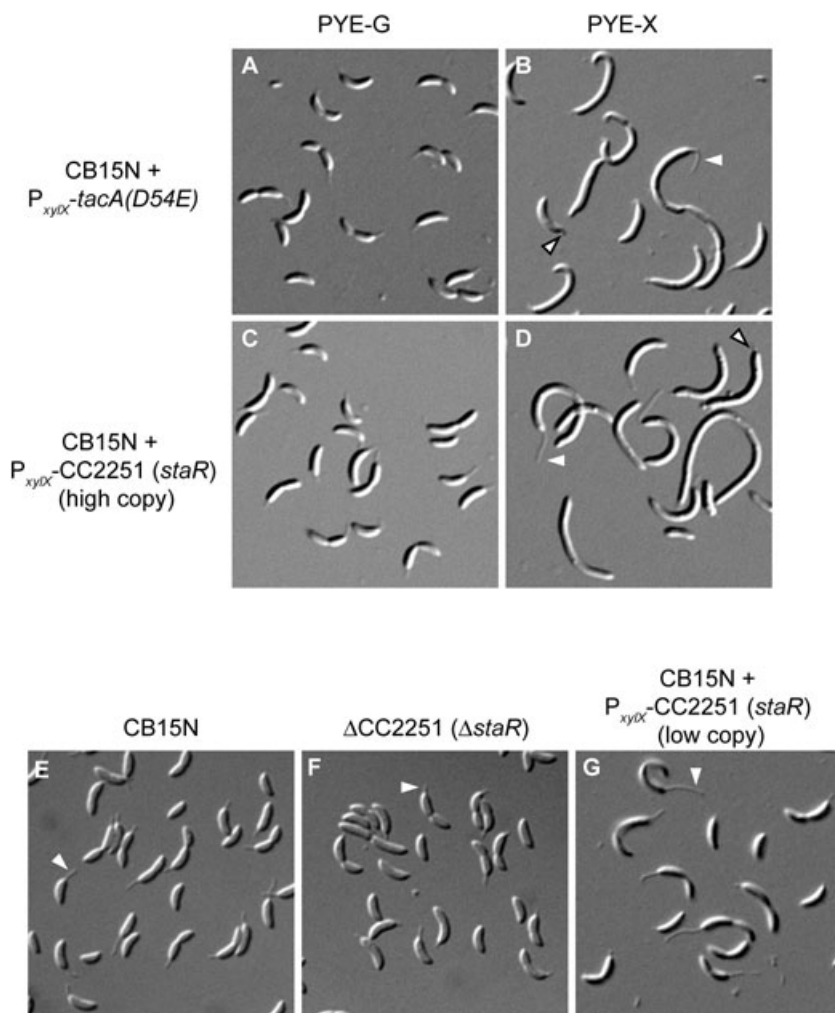


Fig. 5. *staR* (CC2251) is involved in stalk formation.

A–D. Overexpression of *tacA(D54E)* in wild-type *Caulobacter* (CB15N) leads to cell filamentation, and defective stalk formation (A vs. B). Similarly, overexpression of CC2251 leads to filamentation and long stalks (C vs. D). White arrowheads indicate long stalks and open arrowheads indicate defective stalks.

E–G. *StaR* regulates stalk length. DIC images of wild-type CB15N (E) $\Delta CC2251$ (F) and ML760 (CB15N + pLXM-CC2251) in PYE xylose (G) for comparison of stalk length. The deletion mutant $\Delta CC2251$ has stalks approximately 1/2 the length of wild type, whereas overexpression of CC2251 results in stalks which are about twice the length of wild type (see text for details).

lators, also known as enhancer-binding proteins (EBPs), which typically function to activate σ^{54} -dependent gene expression. σ^{54} is encoded in *Caulobacter* by the gene *rpoN* and is required for both flagellar and stalk biogenesis (Brun and Shapiro, 1992). FlbD was identified as the EBP response regulator which works with σ^{54} in pre-divisional cells to regulate the expression of flagellar genes (Ramakrishnan *et al.*, 1991; Wingrove *et al.*, 1993; Benson *et al.*, 1994; Wingrove and Gober, 1994). Based on our results, we hypothesize that TacA collaborates with σ^{54} to control genes involved in regulating stalk biogenesis. To identify possible target genes, we used whole genome DNA microarrays to interrogate the expression patterns of TacA phosphorelay mutants ($\Delta shkA$, $\Delta shpA$, $\Delta tacA$) and a *rpoN* disruption mutant *rpoN::Tn5* (Fig. 6). To partition the σ^{54} regulon into FlbD-

and TacA-dependent genes, we also examined a $\Delta flbD$ strain (Fig. 6).

Strains were grown to mid-log phase ($OD_{600} \sim 0.4$) in rich medium, then RNA was harvested and used to probe whole-genome DNA microarrays. Each mutant strain was compared with the wild-type CB15N and each comparison done in duplicate or triplicate with results averaged. Genes whose expression level changed at least twofold in *rpoN::Tn5* and in any one of the phosphorelay or *flbD* mutants were selected for further analysis (Fig. 6). Visual inspection of expression profiles for each mutant relative to wild type, clearly demonstrated the similarity of $\Delta shkA$, $\Delta shpA$, $\Delta tacA$ and *rpoN::Tn5* (Fig. 6). Correlation coefficients for each pairwise comparison among these mutants were greater than 0.73. Similarly high correlation coefficients have been seen for mutants of other two-compo-

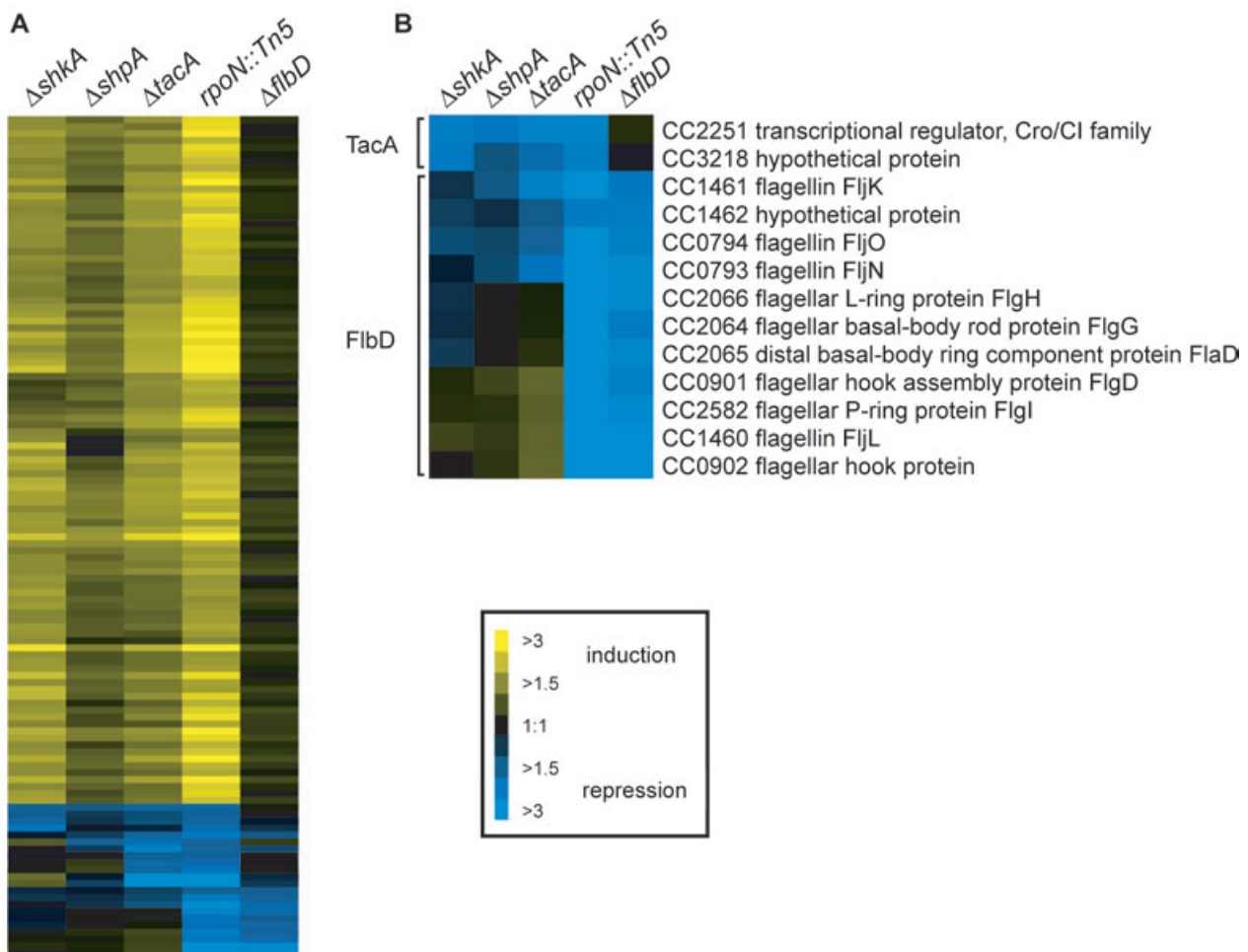


Fig. 6. Expression profiles of $\Delta shkA$, $\Delta shpA$, $\Delta tacA$, *rpoN::Tn5* and $\Delta flbD$. Colours, as indicated in the legend, represent upregulation (yellow) or downregulation (blue) in comparison with expression in wild-type cells.

A. Correlation between expression profiles of $\Delta shkA$, $\Delta shpA$, $\Delta tacA$ (see text for details). Columns, corresponding to $\Delta shkA$, $\Delta shpA$, $\Delta tacA$, *rpoN* mutant and $\Delta flbD$, show only genes upregulated or downregulated more than twofold in at least one of the mutants. For complete data, see Table S1.

B. Genes consistently downregulated in phosphorelay mutants and *rpoN* form a putative TacA regulon, and genes consistently downregulated in *rpoN* and $\Delta flbD$ the FlbD regulon.

nent signalling genes which function in the same pathway (Jacobs *et al.*, 2003). These results thus add further support to the biochemical and genetic data demonstrating that ShkA-ShpA-TacA constitutes a phosphorelay which controls gene expression through phosphorylation of TacA.

We predicted that the TacA target genes involved in stalk biogenesis would be similarly affected in $\Delta shkA$, $\Delta shpA$, $\Delta tacA$ and $rpoN::Tn5$, each of which lacks stalks, but unchanged in the $\Delta flbD$ mutant which is non-motile, but retains stalks. In total, 30 genes satisfied these criteria, two of which are consistently downregulated in each stalkless mutant and 28 upregulated in each. The two downregulated genes contained σ^{54} binding sites (TGGCCN5-TTGC) (Wu *et al.*, 1995) in their upstream regulatory

regions, suggesting that each is a direct target of TacA and σ^{54} . CC3218 has no predicted function based on sequence homology but is transcriptionally cell cycle-regulated (Laub *et al.*, 2000) with expression highest in stalked cells and again in late predivisional cells. The other putative TacA target, CC2251, is predicted to encode a transcription factor of the Cro/C1 family. During wild-type cell cycle progression CC2251 mRNA levels peak in predivisional cells, shortly after *tacA* expression peaks, suggesting that these regulators may form a transcriptional cascade which controls stalk biogenesis (Fig. 7).

Although EBP response regulators such as TacA typically activate gene expression, some can directly repress genes, independent of σ^{54} (Wingrove *et al.*, 1993; Benson *et al.*, 1994; Wingrove and Guber, 1994). Hence to identify

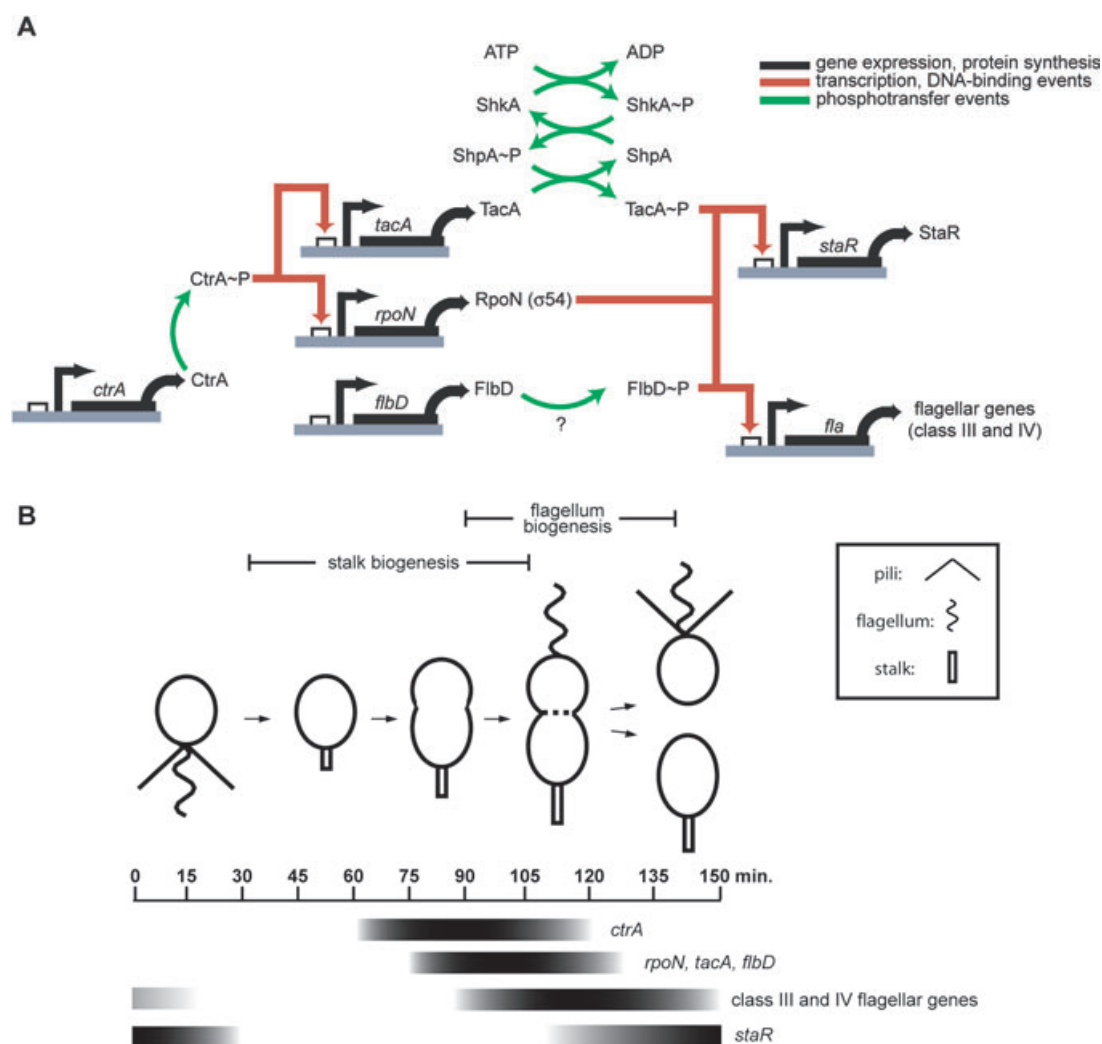


Fig. 7. Model of the genetic circuitry regulating polar morphogenesis in *C. crescentus*.

A. Transcriptional regulation of stalk and flagellar genes. Phosphorylated CtrA activates transcription of *rpoN* (σ^{54}) and *tacA*. σ^{54} and FibD activate transcription of flagellar genes whereas σ^{54} and phosphorylated TacA activate transcription of stalk biogenesis genes including *staR*. A phosphorelay, composed of ShkA (CC0138) and ShpA (CC1114), phosphorylates TacA.

B. Cell cycle-regulated transcription of genes involved in regulation of stalk and flagellum biogenesis (see text for details).

genes which may be directly repressed by TacA, we searched for genes whose expression was significantly upregulated in $\Delta tacA$, but unaffected in the *rpoN* mutant (Table S1). The only gene fitting these criteria was CC3314, which is annotated as a 'conserved hypothetical' and reads divergently from *tacA* itself. All other genes are similarly upregulated in *rpoN::Tn5* and each of the phosphorelay mutants, suggesting that they are regulated indirectly by TacA, perhaps through the transcription factor CC2251. The vast majority of these genes have no annotated function, but their roles, if any, in stalk biogenesis can now be explored.

staR (CC2251) expression is regulated by the TacA phosphorelay and regulates stalk biogenesis

Microarray analysis identified at least two genes, CC2251 and CC3218, as probable direct targets of TacA. To determine their roles, if any, in stalk biogenesis, we constructed deletion and overexpression strains for each gene. Deletion and overexpression of CC3218 had no obvious phenotype (data not shown). Deletion of CC2251 did not eliminate stalks, but the average stalk length for $\Delta CC2251$ cells ($0.68 \mu\text{m} \pm 0.24$, Fig. 5F) was significantly shorter than wild type ($1.26 \mu\text{m} \pm 0.32$, Fig. 5E). Conversely, overexpression of CC2251 from a xylose-inducible promoter on the low-copy vector pMR20 resulted in cells with stalks that were highly variable and longer on average ($1.95 \mu\text{m} \pm 0.89$, Fig. 5G) than wild type. Overexpression of CC2251 from a high-copy (pJS71) vector also produced longer stalks in addition to a growth defect and filamentous cells (Fig. 5D). This growth defect and filamentation was similar to the phenotype of TacA(D54E) overexpression (Fig. 5B), consistent with CC2251 being a direct target of TacA. Based on these observations we have named CC2251 *staR* for stalk biogenesis regulator. We note though, that because $\Delta CC2251$ does not precisely phenocopy $\Delta tacA$, there must be other TacA target genes which also help to control stalk biogenesis. Candidates from the DNA microarray data will need to be examined to fully account for the stalkless phenotype of *tacA*, *shkA* and *shpA* mutants.

Discussion

Stalk biogenesis in Caulobacter

For *Caulobacter*, a developmental program is tightly coupled to cell cycle progression. This development includes three major morphogenetic events, biogenesis of a flagellum, polar pili and a stalk. While the regulation of flagellum assembly and, to a lesser extent, pili biogenesis have been worked out in mechanistic detail (Gober and England, 2000; Skerker and Shapiro, 2000; Viollier *et al.*,

2002a,b), the regulation of stalk biogenesis has remained poorly understood. Here, we have identified a key signal transduction pathway responsible for stalk formation during the cell cycle and have begun outlining the transcriptional pathways involved. This genetic circuitry is summarized in Fig. 7A.

At the heart of this model is σ^{54} which is necessary for both flagellum and stalk biogenesis. As in other bacteria, σ^{54} -dependent gene expression in *Caulobacter* requires an activator of the NtrC-family of response regulators, also known as enhancer-binding-proteins, or EBPs. Typically, phosphorylation of an EBP enables it to stimulate the closed-to-open complex transition of a promoter bound by RNA polymerase containing a σ^{54} subunit, thereby coupling activation of the signalling pathway to changes in gene expression (Kustu *et al.*, 1989). The EBP response regulator FliB is induced at the same time as RpoN, and together they regulate genes involved in flagellar biogenesis (Fig. 7B) (Wingrove *et al.*, 1993; Benson *et al.*, 1994; Wingrove and Gober, 1994). We have now identified TacA as the EBP which collaborates with RpoN to regulate genes involved in stalk biogenesis. Furthermore, we identified a phosphorelay which regulates stalk biogenesis by modulating the phosphorylation state of TacA: ShkA, a hybrid histidine kinase, first autophosphorylates and then initiates a phosphorelay in which a phosphoryl group is passed to its own receiver domain, then to the histidine phosphotransferase ShpA, and finally to the transcriptional regulator TacA (Fig. 7).

DNA microarray analysis identified two genes controlled by TacA which may help regulate stalk biogenesis: CC2251 (*staR*) and CC3218. The mRNAs for both *staR* and CC3218 are cell cycle-regulated with induction in late predivisional cells, immediately after the induction of *tacA* (M. T. Laub, unpubl. data) (Fig. 7B). *StaR* appears to play a role in controlling stalk length, as the deletion strain has stalks shorter than wild type, and overexpression leads to longer stalks (Fig. 5). However, as *staR* mutants do not completely lack stalks or exhibit cellular elongation like *tacA* mutants, other TacA targets remain to be identified and characterized. The microarray data presented here can now be explored to find these additional targets.

The coupling of stalk biogenesis to cell cycle progression is accomplished in large part by CtrA, the master cell cycle regulator. CtrA is regulated at multiple levels during cell cycle progression such that activity drops during the G1-S transition and then rapidly returns to peak levels as S phase proceeds (Domian *et al.*, 1997). CtrA triggers both flagellum and stalk biogenesis by directly activating *rpoN* (σ^{54}) and *tacA* (Laub *et al.*, 2002). Taken together, we propose that stalk biogenesis, like flagellum biogenesis, is regulated by a transcriptional cascade: CtrA is induced after DNA replication initiation and directly activates synthesis of σ^{54} and TacA, which together activate

the expression of stalk regulatory genes, including the transcription factor *staR*, which in turn probably controls the expression of yet other genes required for stalk biogenesis.

Precisely how PleC, another histidine kinase required for stalk biogenesis, feeds into the stalk regulatory circuit remains unknown. However, suppressor analyses place CtrA downstream of PleC, suggesting that the effect may be through regulation of CtrA activity (Ohta *et al.*, 1992; Wu *et al.*, 1998).

Stalk biogenesis is a cell cycle-regulated event and initially occurs in only one of the two daughter cells produced by cell division, raising the possibility that TacA activity is controlled spatially as well as temporally. FliB, for example, is phosphorylated and active only in the nascent swarmer cell, where it activates expression of late flagellar genes and represses early flagellar genes (Gober and England, 2000). In the nascent stalked cell, FliB is present but inactive; this pool of FliB will be activated as the stalked cell develops, initiating early flagellar gene expression in the predivisional cell. Whether TacA activity is also asymmetrically regulated in a manner that restricts stalk biogenesis to a single daughter cell, the stalked cell, remains to be explored.

What signals lead to activation of TacA?

Why does *Caulobacter* use a phosphorelay to control stalk biogenesis? It has been suggested that phosphorelays allow the integration of multiple signals by providing numerous points of control. In *Bacillus subtilis*, a number of signals impinge on the phosphorelay controlling sporulation initiation by affecting the phosphorylation of different pathway components (Perego *et al.*, 1994). Stalk biogenesis is a major developmental event in the life cycle of *Caulobacter*, and hence may also integrate a wide range of signals. However, the nature of the signal(s) controlling the ShkA-ShpA-TacA phosphorelay is not yet known. ShkA is predicted to be a soluble, cytoplasmic kinase, suggesting that the phosphorelay may respond to an internal cell cycle cue. *Caulobacter* thus appears to have at least two independent pathways for regulating stalk biogenesis, one dependent on an external cue, phosphate starvation, and one linked to cell cycle progression.

Identification of a histidine phosphotransferase

ShkA-ShpA-TacA is the first phosphorelay identified in *C. crescentus* as ShpA is the first histidine phosphotransferase identified in this organism. The *C. crescentus* genome likely encodes other histidine phosphotransferases. CC1220, identified here in the same computational screen as ShpA, is one candidate, but others almost

certainly exist, particularly given that the *Caulobacter* genome encodes 27 hybrid histidine kinases. Hybrid kinases often function in phosphorelays like the one described here; however, in some cases the C-terminal receiver domain of a hybrid kinase may function as an auto-inhibitory domain. Intramolecular phosphorylation may relieve this inhibition, allowing the kinase to phosphorylate another, diffusible response regulator, as with the *Agrobacterium tumefaciens* hybrid kinase VirA (Chang *et al.*, 1996).

Rapid, systematic mapping of complex phosphorylation cascades

To identify the probable *in vivo* cognate substrates for ShpA, we adapted a technique called phosphotransfer profiling (Skerker *et al.*, 2005). By examining phosphotransfer from a kinase to each response regulator in parallel, and at multiple time points, kinetic preference is revealed and identifies the probable *in vivo* targets of the kinase (Skerker *et al.*, 2005). Here, we hypothesized that histidine phosphotransferases would similarly exhibit a kinetic preference with respect to both soluble response regulators and the receiver domains of hybrid histidine kinases. A previous smaller scale study of two phosphorelays also suggested that histidine phosphotransferases exhibit kinetic preference *in vitro* (Perraud *et al.*, 1998). Our phosphotransfer profiling experiments indeed demonstrated a kinetic preference for ShpA to transfer phosphoryl groups to or from the receiver domains of ShkA and TacA. Our genetic analyses (Figs 3 and 4) and DNA microarray results (Fig. 6) confirmed the *in vivo* relevance of these interactions. We suggest that histidine phosphotransferases in general may exhibit a global kinetic preference for interaction with their cognate substrates, similar to what has been observed for histidine kinases.

The global kinetic preference of histidine kinases for their cognate response regulator substrates means that the specificity of two-component signal transduction pathways is determined largely at a biochemical level; other factors probably function primarily to enhance this inherent specificity. Our results with ShpA suggest that these observations extend to histidine phosphotransferases and are general properties of two-component signalling pathways. We thus anticipate that our phosphotransfer profiling technique will be generally applicable to the mapping of phosphorelays, both in *Caulobacter* as well as in other organisms. Two-component signalling systems are prevalent throughout the bacterial kingdom as well as being present in fungi and plants (Stock *et al.*, 2000), and the mapping of pathway connectivity among large numbers of signalling components remains a major challenge.

Concluding remarks

Many organisms couple developmental programs and morphogenesis to cell cycle progression. In the budding yeast *S. cerevisiae*, mating requires a morphological change called shmooing which prepares haploid cells for fusion. This morphological event is tied to cell cycle progression and can only occur during G1 phase. For *B. subtilis* the initiation of sporulation, a complex developmental program, is also tightly coupled to cell cycle events (Burkholder *et al.*, 2001). The morphological events of flagellar, pili and stalk biogenesis in *Caulobacter* are similarly dependent on cell cycle progression. The identification of a complete signalling pathway controlling stalk biogenesis now opens the way to a more complete understanding of how this key morphological event is regulated in space and time during the *Caulobacter* cell cycle.

Experimental procedures

Bacterial strains, plasmids and growth conditions

Caulobacter crescentus strains were grown in peptone-yeast extract (PYE, rich medium) or M2G (minimal medium) at 30°C (Ely, 1991), supplemented with 3% sucrose, tetracycline (1 µg ml⁻¹), kanamycin (25 µg ml⁻¹), spectinomycin (25 µg ml⁻¹), 0.1% glucose, or 0.1% xylose, as required. Low-phosphate growth experiments were performed as previously described (Quon *et al.*, 1996). *E. coli* strains were grown at 30°C or 37°C in Luria–Bertani broth supplemented with carbenicillin (100 µg ml⁻¹), chloramphenicol (30 µg ml⁻¹), tetracycline (10 µg ml⁻¹), kanamycin (50 µg ml⁻¹) or spectinomycin (50 µg ml⁻¹) as necessary. PYE swarm plates contained 0.3% bacto agar. Plasmids were transformed into *C. crescentus* by electroporation. Tetracycline marked deletion strains for CC1114, CC2251 and CC3218 were generated by a two-step recombination protocol (Skerker *et al.*, 2005). pENTR clones of the 27 hybrid kinase receiver domains were constructed as previously described (Skerker *et al.*, 2005). For *in vivo* expression of *Caulobacter* genes, pENTR plasmids for CC0138, CC1114, CC1114 (H56A), TacA, TacA(D54E), CC2251 and CC3218 were recombined with either a high-copy destination vector pHXM-DEST or a low-copy destination vector pLXM-DEST (Table S2), as necessary, to generate xylose-inducible constructs (Table S2). For overexpression experiments in *Caulobacter*, using pHXM-based vectors, saturated overnight cultures grown in PYE plus glucose were washed twice in PYE medium and then diluted to OD₆₀₀ = 0.03 in either PYE plus glucose or xylose. For experiments using the low copy vector pLXM-CC2251 samples were grown overnight in PYE plus xylose prior to analysis.

Strains and plasmids generated are listed in Table S2. Primers and plasmids used to generate deletion strains, pENTR clones and point mutations are listed in Table S3. Site-directed mutagenesis was performed using the QuikChange protocol (Stratagene), with pENTR clones as templates. Morphology of mid-log phase cultures was imaged as described previously using DIC microscopy

(Skerker *et al.*, 2005). Stalks were visualized by staining with 5 µM Syto-9 (Molecular Probes).

Sequence analysis and homology modelling

Alpha-helical content was estimated using the Garnier algorithm within EMBOSS (<http://emboss.sourceforge.net>). A structure-based multiple sequence alignment of CC1114 against other known phosphotransferases was constructed using 3D-Coffee (Poirot *et al.*, 2004). This alignment was used as input to Swiss-Model (Schwede *et al.*, 2003) to predict the structure of CC1114 using the following templates: ArcB (PDB: 1FR0), Ypd1 (PDB: 1QSP) and LuxU (PDB: 1Y6D). ArcB provided the best alignment and the predicted CC1114 structure was analysed and displayed using UCSF Chimera (Pettersen *et al.*, 2004).

Gateway cloning and protein purification

Escherichia coli thioredoxin (TRX)-His₆ expression plasmids for all 44 response regulators and 27 hybrid kinase receiver domains were generated using recombinational cloning and purified as described previously (Skerker *et al.*, 2005). CC1114 and CC1114(H56A) were expressed and purified as N-terminal His₆-tagged proteins using the destination vector, pHIS-DEST. To construct pHIS-DEST, pET15b (Novagen) was digested with NdeI, blunted with T4 DNA polymerase, and the RfC Gateway vector conversion cassette (Invitrogen) was inserted. A His₆-version of the TacA receiver domain (TacA-RD) was also constructed and purified, using pHIS-DEST. TacA-RD yielded a cleaner purification, and acted identical to full-length TacA in our assays, so we substituted this protein as necessary. Entry clones of the kinase domains of CckA, CC0138, CC3102 were recombined into pTRX-HIS-DEST or pHIS-MBP-DEST (for CC3219), and purified as either TRX-His₆ or His₆-MBP fusions. All purified proteins were stored in HKEDG buffer (10 mM HEPES-KOH, pH 8.0, 50 mM KCl, 10% glycerol, 0.1 mM EDTA, 1 mM DTT) and concentrations were normalized by densitometry.

Phosphotransfer profiling and phosphorelay biochemistry

We used a modified phosphotransfer profiling method (Skerker *et al.*, 2005) to identify the cognate substrates for CC1114 (Fig. 2C and D, Fig. S2). All reactions and dilutions were performed in HKEDG buffer plus 5 mM MgCl₂. First, we generated CC1114~P by incubating 10 µM His₆-CC1114 with 1 µM TRX-His₆-CC0138-HK and 1 µM TRX-His₆-CC0138-RD plus 1 µCi µl⁻¹ [³²P]ATP (~6000 Ci mmol⁻¹, Amersham Biosciences) for 30 min at 30°C. This reaction was then diluted 10-fold, and 5 µl of the mixture was added to 5 µl of buffer alone (as a control) or 5 µl of each purified response regulator or hybrid receiver domain (diluted to 5 µM) with incubations for 2 min at room temperature. The final concentrations were 0.5 µM for CC1114, and 2.5 µM for the phosphotransfer substrates. To demonstrate phosphorylation of CC1114 by various hybrid kinases (Fig. 2A), the following four autophosphorylation reactions (30 µl total volume) were performed: (i) TRX-His₆-CckA (6 µM), (ii) TRX-His₆-CC0138-HK (0.5 µM), (iii) TRX-His₆-CC3102-HK (4.5 µM), or (iv) His₆-MBP-

CC3219-HK (20 μ M) were incubated for 30 min at 30°C after addition of 30 μ Ci [γ - 32 P]ATP. Then, 1 μ l of reaction A, 1 μ l of reaction B, 4 μ l of reaction C, and 9 μ l of reaction D were mixed with 1 μ M of the corresponding receiver domains of each histidine kinase, and, as necessary, with 10 μ M of His₆-CC1114 for 2 or 5 min, in a total volume of 10 μ l. For analysis of CC1114 activity (Fig. 2B), reactions were performed the same as for phosphotransfer profiling except that various components were omitted before incubating 30 min at 30°C. For analysis of the complete TacA phosphorelay and kinetics (Fig. 2E and G), CC1114~P was prepared as above, diluted, and then mixed with 5 μ l of 5 μ M His₆-TacA-RD or other hybrid kinase receiver domains. All phosphotransfer reactions were stopped with 3.5 μ l of 4 \times SDS-PAGE sample buffer and analysed using 12% or 15% Tris-HCl gels as described previously (Skerker *et al.*, 2005).

Microarray analysis of the *TacA* regulon

Strains were grown in PYE and harvested at OD₆₀₀ = 0.4. RNA preparation was performed using the RNA-easy Kit (Qiagen). DNA arrays contained 50mer probes for each gene in the *Caulobacter* genome (see Table S1 for sequences). Three or more independent cultures were used for each experiment and each sample was labelled either with Cy5-dCTP or Cy3-dCTP (Amersham Biosciences). Hybridizations, scanning and data processing were performed as described previously (Laub *et al.*, 2002) except that hybridizations contained 30% formamide and were incubated at 44°C for 6 h.

Acknowledgements

We gratefully acknowledge support from the Office of Science (BER), US Department of Energy, Grants No. DE-FG03-01ER63219 and DE-FG02-04ER63922. Support also provided in part by a National Institutes of Health grant to M.T.L. and the Bauer Center for Genomics Research at Harvard University.

References

Benson, A.K., Ramakrishnan, G., Ohta, N., Feng, J., Ninfa, A.J., and Newton, A. (1994) The *Caulobacter crescentus* FibD protein acts at *ftt* sequence elements both to activate and to repress transcription of cell cycle-regulated flagellar genes. *Proc Natl Acad Sci USA* **91**: 4989–4993.

Brun, Y.V., and Shapiro, L. (1992) A temporally controlled sigma-factor is required for polar morphogenesis and normal cell division in *Caulobacter*. *Genes Dev* **6**: 2395–2408.

Burkholder, W.F., Kurtser, I., and Grossman, A.D. (2001) Replication initiation proteins regulate a developmental checkpoint in *Bacillus subtilis*. *Cell* **104**: 269–279.

Chang, C.H., Zhu, J., and Winans, S.C. (1996) Pleiotropic phenotypes caused by genetic ablation of the receiver module of the *Agrobacterium tumefaciens* VirA protein. *J Bacteriol* **178**: 4710–4716.

Domian, I.J., Quon, K.C., and Shapiro, L. (1997) Cell type-specific phosphorylation and proteolysis of a transcrip-

tional regulator controls the G1-to-S transition in a bacterial cell cycle. *Cell* **90**: 415–424.

Ely, B. (1991) Genetics of *Caulobacter crescentus*. *Methods Enzymol* **204**: 372–384.

Georgellis, D., Kwon, O., De Wulf, P., and Lin, E.C. (1998) Signal decay through a reverse phosphorelay in the Arc two-component signal transduction system. *J Biol Chem* **273**: 32864–32869.

Gober, J.W., and England, J.C. (2000) Regulation of flagellum biosynthesis and motility in *caulobacter*. In *Prokaryotic Development*. Brun, Y.V., and Shimkets, L.J. (eds). Washington, DC: American Society for Microbiology Press, pp. 319–339.

Gonin, M., Quardokus, E.M., O'Donnol, D., Maddock, J., and Brun, Y.V. (2000) Regulation of stalk elongation by phosphate in *Caulobacter crescentus*. *J Bacteriol* **182**: 337–347.

Hoch, J.A., and Silhavy, T.J. (eds). (1995) *Two-Component Signal Transduction*. Washington, DC: American Society for Microbiology Press.

Jacobs, C., Ausmees, N., Cordwell, S.J., Shapiro, L., and Laub, M.T. (2003) Functions of the CckA histidine kinase in *Caulobacter* cell cycle control. *Mol Microbiol* **47**: 1279–1290.

Kato, M., Mizuno, T., Shimizu, T., and Hakoshima, T. (1997) Insights into multistep phosphorelay from the crystal structure of the C-terminal HPT domain of ArcB. *Cell* **88**: 717–723.

Klose, K.E., Weiss, D.S., and Kustu, S. (1993) Glutamate at the site of phosphorylation of nitrogen-regulatory protein NTRC mimics aspartyl-phosphate and activates the protein. *J Mol Biol* **232**: 67–78.

Kurtz, H.D., Jr, and Smit, J. (1994) The *Caulobacter crescentus* holdfast: identification of holdfast attachment complex genes. *FEMS Microbiol Lett* **116**: 175–182.

Kustu, S., Santero, E., Keener, J., Popham, D., and Weiss, D. (1989) Expression of sigma 54 (*ntrA*)-dependent genes is probably united by a common mechanism. *Microbiol Rev* **53**: 367–376.

Laub, M.T., McAdams, H.H., Feldblyum, T., Fraser, C.M., and Shapiro, L. (2000) Global analysis of the genetic network controlling a bacterial cell cycle. *Science* **290**: 2144–2148.

Laub, M.T., Chen, S.L., Shapiro, L., and McAdams, H.H. (2002) Genes directly controlled by CtrA, a master regulator of the *Caulobacter* cell cycle. *Proc Natl Acad Sci USA* **99**: 4632–4637.

Meisenzahl, A.C., Shapiro, L., and Jenal, U. (1997) Isolation and characterization of a xylose-dependent promoter from *Caulobacter crescentus*. *J Bacteriol* **179**: 592–600.

Nierman, W.C., Feldblyum, T.V., Laub, M.T., Paulsen, I.T., Nelson, K.E., Eisen, J., *et al.* (2001) Complete genome sequence of *Caulobacter crescentus*. *Proc Natl Acad Sci USA* **98**: 4136–4141.

Ohta, N., Lane, T., Ninfa, E.G., Sommer, J.M., and Newton, A. (1992) A histidine protein kinase homologue required for regulation of bacterial cell division and differentiation. *Proc Natl Acad Sci USA* **89**: 10297–10301.

Ohta, N., Grebe, T.W., and Newton, A. (2000) Signal transduction and cell cycle checkpoints in developmental regulation of *Caulobacter*. In *Prokaryotic Development*. Brun,

- Y.V., and Shimkets, L.J. (eds). Washington, DC: American Society for Microbiology Press, pp. 341–359.
- Perego, M., Hanstein, C., Welsh, K.M., Djavakhishvili, T., Glaser, P., and Hoch, J.A. (1994) Multiple protein-aspartate phosphatases provide a mechanism for the integration of diverse signals in the control of development in *B. subtilis*. *Cell* **79**: 1047–1055.
- Perraud, A.L., Kimmel, B., Weiss, V., and Gross, R. (1998) Specificity of the BvgAS and EvgAS phosphorelay is mediated by the C-terminal HPT domains of the sensor proteins. *Mol Microbiol* **27**: 875–887.
- Pettersen, E.F., Goddard, T.D., Huang, C.C., Couch, G.S., Greenblatt, D.M., Meng, E.C., and Ferrin, T.E. (2004) UCSF Chimera – a visualization system for exploratory research and analysis. *J Comput Chem* **25**: 1605–1612.
- Poindexter, J.S. (1964) Biological properties and classification of the *Caulobacter* group. *Bacteriol Rev* **28**: 231–295.
- Poindexter, J.S. (1978) Selection for nonbuoyant morphological mutants of *Caulobacter crescentus*. *J Bacteriol* **135**: 1141–1145.
- Poindexter, J.S. (1984) The role of calcium in stalk development and in phosphate acquisition in *Caulobacter crescentus*. *Arch Microbiol* **138**: 140–152.
- Poirot, O., Suhre, K., Abergel, C., O'Toole, E., and Notredame, C. (2004) 3DCoffee@igs: a web server for combining sequences and structures into a multiple sequence alignment. *Nucleic Acids Res* **32**: W37–W40.
- Quon, K.C., Marczyński, G.T., and Shapiro, L. (1996) Cell cycle control by an essential bacterial two-component signal transduction protein. *Cell* **84**: 83–93.
- Ramakrishnan, G., Zhao, J.L., and Newton, A. (1991) The cell cycle-regulated flagellar gene *flbF* of *Caulobacter crescentus* is homologous to a virulence locus (*lcrD*) of *Yersinia pestis*. *J Bacteriol* **173**: 7283–7292.
- Ramakrishnan, G., Zhao, J.L., and Newton, A. (1994) Multiple structural proteins are required for both transcriptional activation and negative autoregulation of *Caulobacter crescentus* flagellar genes. *J Bacteriol* **176**: 7587–7600.
- Ryan, K.R., and Shapiro, L. (2003) Temporal and spatial regulation in prokaryotic cell cycle progression and development. *Annu Rev Biochem* **72**: 367–394.
- Schwede, T., Kopp, J., Guex, N., and Peitsch, M.C. (2003) SWISS-MODEL: an automated protein homology-modeling server. *Nucleic Acids Res* **31**: 3381–3385.
- Skerker, J.M., and Shapiro, L. (2000) Identification and cell cycle control of a novel pilus system in *Caulobacter crescentus*. *EMBO J* **19**: 3223–3234.
- Skerker, J.M., and Laub, M.T. (2004) Cell-cycle progression and the generation of asymmetry in *Caulobacter crescentus*. *Nat Rev Microbiol* **2**: 325–337.
- Skerker, J.M., Prasol, M.S., Perchuk, B.S., Biondi, E.G., and Laub, M.T. (2005) Two-component signal transduction pathways regulating growth and cell cycle progression in a bacterium: a system-level analysis. *PLoS Biol* **3**: e334.
- Smith, C.S., Hinz, A., Bodenmiller, D., Larson, D.E., and Brun, Y.V. (2003) Identification of genes required for synthesis of the adhesive holdfast in *Caulobacter crescentus*. *J Bacteriol* **185**: 1432–1442.
- Sommer, J.M., and Newton, A. (1989) Turning off flagellum rotation requires the pleiotropic gene *pleD*: *pleA*, *pleC*, and *pleD* define two morphogenic pathways in *Caulobacter crescentus*. *J Bacteriol* **171**: 392–401.
- Song, H.K., Lee, J.Y., Lee, M.G., Moon, J., Min, K., Yang, J.K., and Suh, S.W. (1999) Insights into eukaryotic multi-step phosphorelay signal transduction revealed by the crystal structure of Ypd1p from *Saccharomyces cerevisiae*. *J Mol Biol* **293**: 753–761.
- Stock, A.M., Robinson, V.L., and Goudreau, P.N. (2000) Two-component signal transduction. *Annu Rev Biochem* **69**: 183–215.
- Uhl, M.A., and Miller, J.F. (1996) Central role of the BvgS receiver as a phosphorylated intermediate in a complex two-component phosphorelay. *J Biol Chem* **271**: 33176–33180.
- Ulrich, D.L., Kojetin, D., Bassler, B.L., Cavanagh, J., and Loria, J.P. (2005) Solution structure and dynamics of LuxU from *Vibrio harveyi*, a phosphotransferase protein involved in bacterial quorum sensing. *J Mol Biol* **347**: 297–307.
- Viollier, P.H., Sternheim, N., and Shapiro, L. (2002a) Identification of a localization factor for the polar positioning of bacterial structural and regulatory proteins. *Proc Natl Acad Sci USA* **99**: 13831–13836.
- Viollier, P.H., Sternheim, N., and Shapiro, L. (2002b) A dynamically localized histidine kinase controls the asymmetric distribution of polar pili proteins. *EMBO J* **21**: 4420–4428.
- Wagner, J.K., Galvani, C.D., and Brun, Y.V. (2005) *Caulobacter crescentus* requires RodA and MreB for stalk synthesis and prevention of ectopic pole formation. *J Bacteriol* **187**: 544–553.
- Wingrove, J.A., and Gober, J.W. (1994) A sigma 54 transcriptional activator also functions as a pole-specific repressor in *Caulobacter*. *Genes Dev* **8**: 1839–1852.
- Wingrove, J.A., Mangan, E.K., and Gober, J.W. (1993) Spatial and temporal phosphorylation of a transcriptional activator regulates pole-specific gene expression in *Caulobacter*. *Genes Dev* **7**: 1979–1992.
- Wu, J., Benson, A.K., and Newton, A. (1995) Global regulation of a sigma 54-dependent flagellar gene family in *Caulobacter crescentus* by the transcriptional activator FlbD. *J Bacteriol* **177**: 3241–3250.
- Wu, J., Ohta, N., and Newton, A. (1998) An essential, multi-component signal transduction pathway required for cell cycle regulation in *Caulobacter*. *Proc Natl Acad Sci USA* **95**: 1443–1448.
- Xu, Q., and West, A.H. (1999) Conservation of structure and function among histidine-containing phosphotransfer (HPT) domains as revealed by the crystal structure of YPD1. *J Mol Biol* **292**: 1039–1050.

Supplementary material

The following supplementary material is available for this article online:

Fig. S1. Alignment of putative CC1114 orthologues from various alpha-proteobacteria. Putative CC1114 orthologues were identified by reciprocal best BLAST analysis. A multiple sequence alignment was performed using T-COFFEE and drawn using BOXSHADE. Conserved residues are shaded black and marked with an asterisk. Residues which are similar are shaded grey and marked by a period. The sequences

were obtained from the following genomes: *Agrobacterium tumefaciens* C58 (gi17935249), *Sinorhizobium meliloti* 1021 (gi15074749), *Bradyrhizobium japonicum* USDA 110 (gi27380997), *Rhodopseudomonas palustris* CGA009 (gi39937018) and *Caulobacter crescentus* CB15 (gi25399659). Sequences GenBank accession numbers are in parenthesis.

Fig. S2. Phosphotransfer profiling method applied to histidine phosphotransferases.

A. Reactions involved in phosphotransfer profiling.

B. Schematic of phosphotransfer profiling method as applied to histidine phosphotransferases (HPTs).

Fig. S3. Purification of the receiver domains from all 27 hybrid kinases encoded in the *Caulobacter* genome SDS-PAGE analysis of purified TRX-His₆-TEV fusions to each of the 27 receiver domains derived from hybrid kinases (see

Experimental procedures and Table S2). A molecular weight ladder is marked with sizes in kDa. Approximately 500 ng of purified receiver domain was analysed and normalized against an equivalent amount of BSA. Gene names are indicated by their CC number and the predicted molecular weight of each fusion is indicated in Daltons. Six of the 27 receiver domains purified poorly (CC0723, CC0921, CC2521, CC2632, CC3191, CC3560), although a band corresponding to the correct molecular weight is still present in each case.

Table S1. DNA microarray data and probes.

Table S2. Strains and plasmids.

Table S3. Primers for generating pENTR clones, deletion strains and site-directed mutants.

This material is available as part of the online article from <http://www.blackwell-synergy.com>